Design and commissioning of a UHV sputter system for the fabrication of superconducting TiN KID's using High Power Impulse Magnetron Sputtering

C.S. Woodhead, M. Tapia, C. Dunscombe, T. Brien, M. Baghoria, S. Doyle, P. Hargrave
School of Physics and Astronomy, Cardiff University, Cardiff, Wales, UK, CF24 3AA

E-mail: woodheadc@cardiff.ac.uk

Abstract

Titanium nitride (TiN) is an ideal material for fabricating Kinetic Inductance Detectors (KIDs), firstly due to its relatively high and tuneable critical temperature, and secondly its high normal-state resistivity, which allows for a large kinetic inductance and responsivity. However, fabricating large arrays on wafers greater than 150 mm can be challenging due to TiN films being very sensitive to changes in stoichiometry, thickness and contaminants. In this paper we demonstrate a novel technique for making high quality films of superconducting TiN via the use of a high impulse magnetron sputtering technique (HIPIMs) in conjunction with a custom built ultra-high vacuum environment. We detail the design principles of the UHV-HIPIMS sputter system and show that films of high uniformity suitable for use in KID arrays can be achieved.

Introduction

Kinetic Inductance Detectors (KIDs) are a type of superconducting resonator which can be used to detect wavelengths of a broad spectrum from microwaves to x-rays[1]. Their large multiplexing capability and high broadband sensitivity make them an excellent choice for a range of imaging applications from astronomy observations to Terahertz security scanners[2]. In the last few years cameras containing these devices have gone from 1000+ pixels, to 25,000 pixels[3], [4], dramatically improving the quality of the images produced. In addition, higher superconducting transition temperature (Tc) films such as Nb/NbN and TiN are being increasingly used as materials for KID arrays in high background applications e.g. spectrometers[5]. These higher Tc materials can help to simplify the cryogenic cooling requirements, making the camera significantly cheaper to produce compared to lower Tc materials such as Al.

However, depositing these materials on 150 – 200 mm wafers required accommodate this many pixels, whilst maintaining consistent stoichiometry and thickness across the wafer is challenging, due to several factors:

- Variations in thickness by even a few nm can have a large impact on the Tc of very thin films[6].
- Contamination of the film by elements such as oxygen can have a large effect on the quality of a superconductor, with TiN being particularly susceptible[7]. In fact, TiN can be used as a diffusion barrier for Si because of its effectiveness at absorbing contaminates[8].
- Compound materials like TiN require reactive sputtering, which causes compound formation on the target known as "poisoning." This makes the process very difficult to control, with responses to any change in deposition parameters showing significant non-linearity and hysteresis.[9]
- For KID arrays, films with a consistent Tc and kinetic inductance across them is of uttermost importance as any variations can cause resonance shifts which can dramatically reduce the number of working pixels in an array[10].

The goal of this work was to design and build a sputter system capable of depositing uniform films of TiN onto 150 – 200 mm wafers to support the next generation of KID based devices. We present the design principles for building our own Ultra High Vacuum (UHV) system and introduce HIPIMs sputtering and how it can help in the deposition of TiN.

HIPIMs

HIPIMs is a sputtering method utilising intense, brief pulses in the 10s to 100 µs range. This creates high peak currents and strong material ionisation, whilst keeping the average power low relative to DC or pulsed-DC deposition; a comparison of these can be seen in Figure 1. The advantages of this high ionisation are smoother, denser films with increased film adhesion, as well as a high degree of control over the growth orientation, optical and mechanical properties [11]. This high degree of control makes it an excellent choice for reactive applications, e.g. TiN, where the head rapidly transitions from a metallic state (i.e. pure metal) to a poisoned state where the target is covered by a compound. This can be achieved with adjustment of the on/off time of the plasma enabling a high degree of control of the poisoned state of the target and, in some cases, can allow controlled tuning of the crystalline orientation[12]. HIPIMs has already been shown to be well suited for depositing TiN, with thin films of sufficient quality for use as waveguides and plasmonic being previously demonstrated[7], [13]. For superconducting applications HIPIMs sputtering has already shown great promise for coating superconducting Nb onto Cu [14], [15], with reports of higher T_c and denser films over DC sputtering [16]. In HIPIMS the kinetic energy (E_k) of ions incident on the substrate is very high relative to DC, leading to an effective increase in substrate temperature[11], [12]; this has been shown to be a key parameter for superconducting films[15].

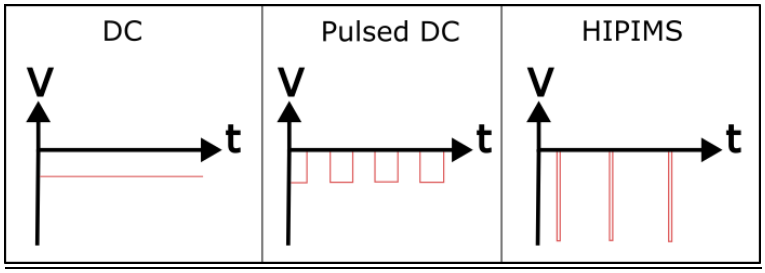

Figure 1: Sketches showing the difference between the bias applied to the head in DC/ DC pulsed sputtering compared to HIPIMs.

Sputter system design

Magnetron

To guarantee thickness uniformity across an 200 mm wafer, a linear magnetron was chosen over a circular one. This enabled the wafer to be scanned across the head, allowing each point of the wafer to see the same plasma conditions for the same amount of time (Figure 2a), a technique often used in industrial coaters. The sputter head chosen was an Angstrom Science unbalanced rectangular UHV magnetron with a 400 x 50 mm target. It can be noted that the head size was chosen to be oversized, in the long dimension, with respect to the wafer, to ensure film uniformity. Linear heads have one long strip of magnets running down their centre, boxed by another set of magnets, forming a racetrack. At the ends of the rectangular head, the magnetic field strengthens and bends around 180° which signifies a discontinuity in the magnetic field which, in turn, effects the plasma in that area and thus the growth of the film. It was therefore decided to oversize the sputter head to ensure that the wafer only encounters the highly uniform centre where the central magnets are located; which for this magnetron is a 240 mm span across the centre point of the target. The standard deviation of the field across this region was approximately 1% of the average field, whereas across the whole head, including the edges, it was as high as 7%. The magnetic field was chosen to be unbalanced to help increase the deposition rate.

The target used was composed of Ti at 99.995% purity or better with ferrous materials minimised to <5ppm to minimise the known effect of ferromagnetism breaking cooper pairs[17].

During operation all sputter systems deposit on surfaces other than the wafer, the build-up of which eventually leads to delamination with large pieces of sputtered material dropping away. This leads to a conundrum for the designer of whether to allow flakes to fall towards the wafer contaminating the surface or towards the sputter head leading to target arcing which can also badly effect film quality [18], [19]. In this instance we chose the top-down configuration (target facing down towards the wafer) to ensure the film is as uniform as possible and does not contain implanted liquid metal droplets that get thrown out during an arcing event. Placing it top-down meant gravity drops debris away from the target, which is important as a UHV system is impractical to regularly open and clean.

Vacuum system

When growing films of superconducting TiN it is very important that the oxygen partial pressure is as low as possible to prevent any oxygen incorporation in the film, which can have a detrimental effect on its superconducting properties. To achieve this the system was designed to operate at UHV pressures using stainless-steel chambers with CF flanges; these, in conjunction with baking to remove water vapour help eliminate any contamination from oxygen. To reduce outgassing, internal components such as shields are manufactured from low outgassing materials such as stainless steel, and the use of vent holes and vented screws ensure that trapped air pockets are eliminated. These measures, along with using very high purity targets and sputter gasses (99.999 % or better), minimises the contamination getting into the films.

To make the system 200 mm compatible, the chamber port's internal diameter is 250 mm, with the top port's internal diameter being 500 mm to accommodate the 400 mm-long head. A picture of the growth chamber during operation can be seen in Figure 2b. In addition to the growth chamber, a load-lock and wafer loading system was also used for fast wafer throughput. To ensure the water vapour pumping speed was high a CT8 cryopump was used as the UHV pump, with a turbopump used to pump the load-lock.

The wafer was mounted to a trolley which used vacuum compatible greaseless bearings to move itself along a track and across the head (

Figure 2c). Film thickness could easily be tuned by changing the wafer's velocity. To monitor the process an optical emission spectrometer (OES) was used to monitor the reactive species in the plasma. This linked to the mass flow controllers (MFC), which were programmed to rapidly respond to the OES signal enabling control of the reactive gas. The gas was injected into a bar that runs along the length of the head right next to the target to ensure that the gas enters as close as possible to the target head. This is important, as it has been shown that variations in the distribution and ratio of the reactive gas can lead to variable transition temperatures across the wafer [20], [21]. The pressure of the chamber was measured using a capacitance manometer and controlled by a downstream PID gate valve, which automatically holds the pressure constant.

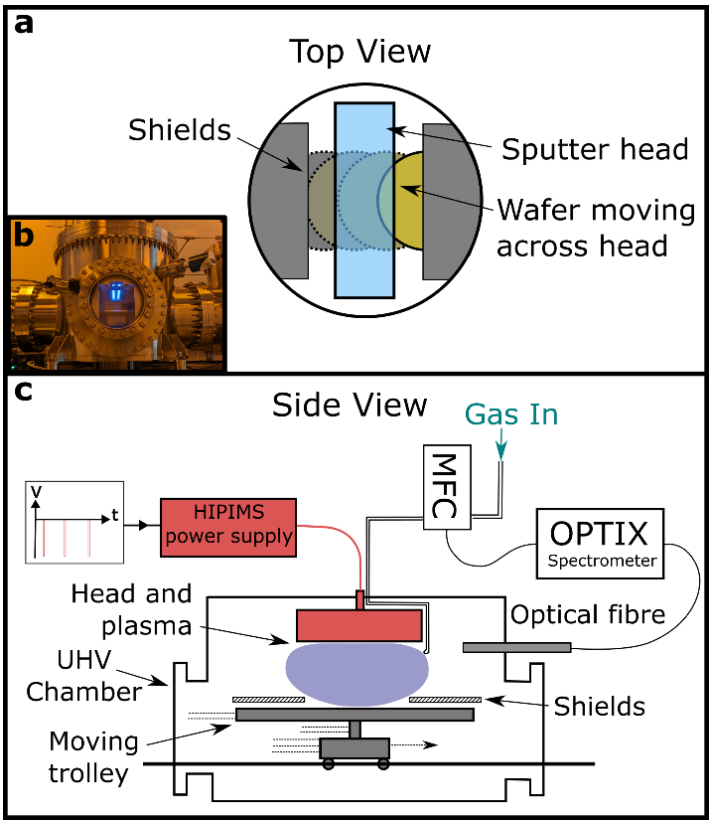

Figure 2: a) Top-down view showing the wafer scanning concept. b) Inset picture showing the growth chamber with plasma ignited. c) Schematic side view showing the sputter system setup.

Initial Results

The assembled sputter system was leak-checked and evacuated to at least $7x10^{-9}$ mbar before depositions commenced. The ultimate pressure the system is capable of reaching after baking is $2x10^{-9}$ mbar. This base pressure of the system is currently limited due to using a non-UHV capable cryopump which is only capable of pumping to this pressure due to KF25 seals present on its backing port. In future, we hope to replace this with metal sealed versions to allow us to reach full UHV pressures.

Titanium nitride was deposited on a 150 mm high resistivity float zone (FZ) wafer at a pressure of $4.3x10^{-3}$ mbar using a Ionautics Hipster 6 HIPIMs power supply, using pulses of 620 V with a width of 40 µs at 420 Hz; the peak current was 85 A giving a power density of 267 Wcm^{-2}. To control the nitrogen content in the film, the system was placed into poisoned mode by slowly changing the nitrogen content in the sputter gas whilst monitoring the titanium emission normalised to the argon emission (Ti/Ar) and the peak current I_{pk}. The results of this are shown in Figure 3, in which three target states are observed; metallic (α), poisoned (γ) and a transition region between the two (β). The different target states can clearly be identified by a change of shape of the pulse current (Figure 3b) from a flattening peak in metal mode, to a sharp triangular peak when poisoned, accompanied by a delay in the current onset. We can also observe in Figure 3a that there is a hysteresis in both the Ti/Ar signal and the I_{pk} between increasing flow and decreasing flow, with the target poisoning at 5 sccm on the way up, and not returning to metallic mode until 0 sccm when reducing flow. This hysteresis is influenced by the rate of change of the Nitrogen flow, and how long it takes the nitrogen to reach the sputter head from the MFC. However, it is also known that target poisoning is a non-linear process and some hysteresis is always present in reactive sputtering[22]. We can also clearly see that the peak current starts to initially drop at a slow rate with the Ti/Ar signal before rapidly reducing as the nitrogen starts to poison the head, at 45 s I_{pk} current starts to rapidly rise until it reaches a maximum of 80 A.

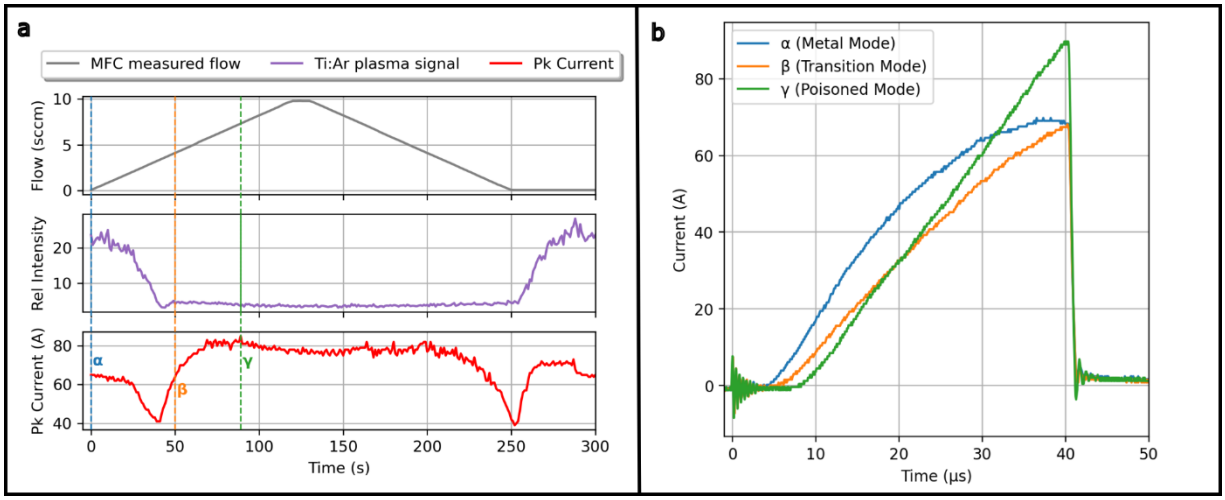

Figure 3: a) Stack plot showing the effect of increasing nitrogen flow (top) on the Titanium plasma emission (middle) and the peak current (bottom). α, β, γ identify different states of the target, metallic state, transitionary state and poisoned respectively, at specific times. The current traces of these are shown in b.

To produce a TiN film we used the OES system to hold the plasma at the point labelled β, so that the ratio of Ti/Ar signal was kept constant throughout the entire 50-minute deposition, which was achieved by a single pass across the head. We found the system would stabilise at this point with a rough N_2:Ar ratio of approximately 1:15.

The films' thicknesses were then characterised using a surface profiler, and their T_c measured using a resistivity measurement in a Quantum Design PPMS system and are shown in Figure 4. The thickness is very consistent with a mean of 81±4.4 nm with no noticeable trend across the wafer. It is notable that the scatter in the readings is nearly all within the uncertainties of the measurement, therefore any radial variation in thickness is less than 8.8 nm.

The T_c measurement of this TiN film is shown inset, with a T_c = 3.402 ± 0.013 K and a RRR = 1.179 and is consistent with several other wafers also studied. The Tc is lower than expected and literature suggests this is potentially due to sub-stoichiometric TiN due to lack of flow nitrogen[20]. However, subsequent attempts to increase this via an increase in nitrogen flow yielded very little change in the overall Tc as well as to the film's

conductivity, which was consistently around 70 Ωcm. Whereas the cause of this low Tc and insensitivity to the flow rate has not been identified, there are two possibilities. The first is that the film contains a significant amount of Ti_2N in its amorphous structure rather than TiN, which is known to suppress the Tc[20]. This could arise from highly energetic Ar ions being reflected away from the target towards the substrate's nitrogen rich TiN surface and preferentially re-sputtering the nitrogen away, a known effect that can occur at low pressures and high energies[7]. Another possibility is that the film contains low levels of contamination that are supressing the Tc (e.g. O). Further study of the crystalline structure of the films and their composition with methods such as x-ray diffraction (XRD), and energy dispersive X-ray spectroscopy (EDX) could help to provide more insight and improve the film quality.

We subsequently decided to assess how suitable these films are for use in MKID arrays. We performed this by etching a simple array of 10 lumped-element KIDs (LEKIDs) with a resonant frequency range of 1-5 GHz and a feedline into the film using a Cl/Ar plasma. These were then cooled down to 80 mK in a dilution refrigerator, so that the resonances could be observed without the bath temperature limiting the resonators performance; one such resonance at 1.95GHz is shown in Figure 5. Designed coupling quality factors (Q_c) of ~ 3000 were reproduced in the measurements, with average intrinsic quality factors (Q_i) = 8700±990 at 80 mK. We found that these LEKIDs were highly responsive to the base temperature under dark conditions (Figure 5), with a continuous resonance shift of >100MHz observed by increasing the temperature from 80 mK to 1.5 K. These Q_i's sit at the low end of MKID arrays discussed in literature with Q_i's from 2,000 to greater than 100,000 being demonstrated[23], [24].

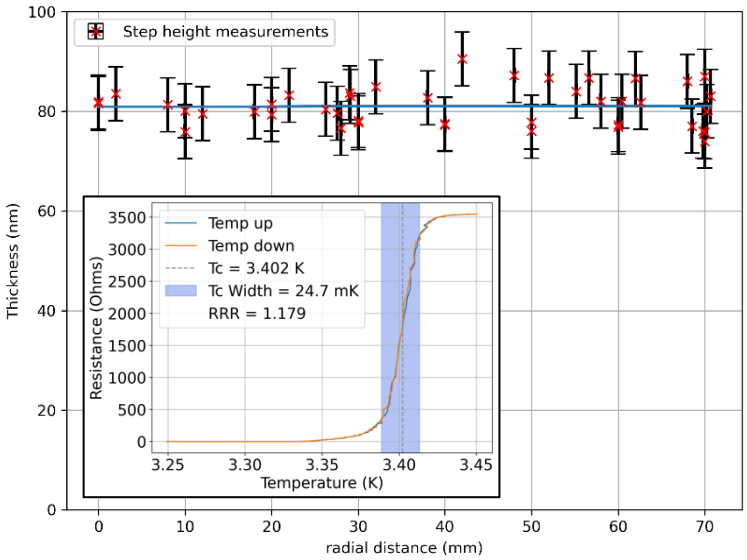

Figure 4: Uniformity across a 150 mm wafer of TiN, Inset: Superconducting transition at Tc = 3.402K

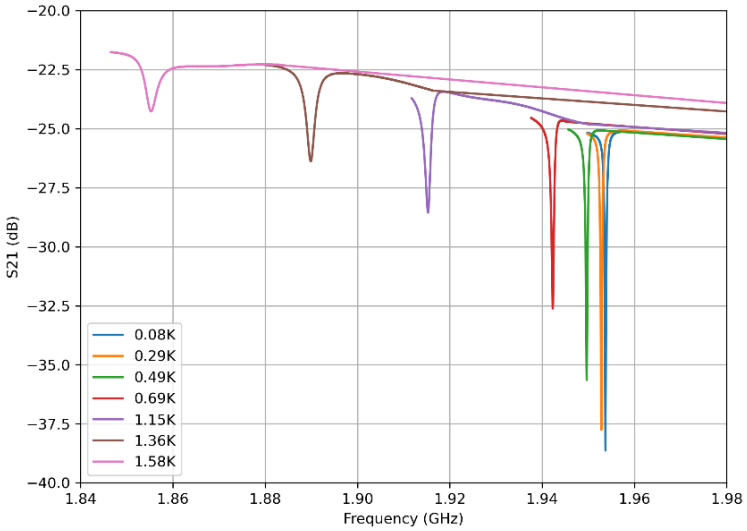

Figure 5: Resonance frequency shift of a 1.953 GHz KID with increasing temperature under dark conditions.

Conclusions

In this paper We have presented a novel approach for creating uniform films of superconducting TiN via the use of a linearly scanning UHV reactive sputter system, which utilises HIPIMs to create superconducting films. The designed system was found to be capable of reaching base pressures of $2x10^{-9}$ mbar, a limit that was due to the use of a non-UHV capable cryopump. With a true UHV cryopump we expect that the system should be capable of reaching the 10^{-10} – 10^{-11} mbar range, which is something we intend to upgrade to in future.

Initial depositions showed that films with thickness uniformity better than 9 nm across a 150 mm wafer can be achieved, with T_c = 3.402 ± 0.013 K and a RRR = 1.179. We also found that resonators patterned into the film show promising results and suggest that, with more development, these films could enable large TiN KID arrays on 150 – 200 mm wafers. The next phase of this work will involve studying the composition of these films to understand the dynamics behind the slightly low transition temperatures. Additionally, we plan to optimise our KID arrays for our film properties, as well as using steps such as wafer surface oxide removal to further improve their performance and reduce noise.

Acknowledgements

This work was funded under a STFC Grant reference ST/V002236/1 “TeraVid - A THz camera for Security & Border Protection Applications. The authors would also like to acknowledge the Institute for Compound Semiconductors (ICS) at Cardiff University for their support and use of their facilities during this project.

References

[1] P. K. Day, H. G. LeDuc, B. A. Mazin, A. Vayonakis, and J. Zmuidzinas, “A broadband superconducting detector suitable for use in large arrays,” *Nature 2003 425:6960*, vol. 425, no. 6960, pp. 817–821, Oct. 2003, doi: 10.1038/nature02037.

[2] G. Ulbricht, M. De Lucia, and E. Baldwin, “Applications for microwave kinetic induction detectors in advanced instrumentation,” *Applied Sciences (Switzerland)*, vol. 11, no. 6, Mar. 2021, doi: 10.3390/app11062671.

[3] J. J. A. Baselmans *et al.*, “A kilo-pixel imaging system for future space based far-infrared observatories using microwave kinetic inductance detectors,” *Astron Astrophys*, vol. 601, p. A89, May 2017, doi: 10.1051/0004-6361/201629653.

[4] L. E. Otal, “The Optical System and the Astronomical Potential of A-MKID, a New Camera Using Microwave Kinetic Inductance Detector Technology,” Rheinischen Friedrich-Wilhelms-Universität Bonn, 2014.
[5] E. Shirokoff *et al.*, “Design and performance of SuperSpec: An on-chip, KID-based, mm-wavelength spectrometer,” *J Low Temp Phys*, vol. 176, no. 5–6, pp. 657–662, Feb. 2014, doi: 10.1007/S10909-014-1122-8/FIGURES/3.
[6] A. Torgovkin, S. Chaudhuri, A. Ruhtinas, M. Lahtinen, T. Sajavaara, and I. J. Maasilta, “High quality superconducting titanium nitride thin film growth using infrared pulsed laser deposition,” *Supercond Sci Technol*, vol. 31, no. 5, p. 055017, Apr. 2018, doi: 10.1088/1361-6668/AAB7D6.
[7] S. Ohya *et al.*, “Room temperature deposition of sputtered TiN films for superconducting coplanar waveguide resonators,” *Supercond Sci Technol*, vol. 27, no. 1, p. 15009, 2013, doi: 10.1088/0953-2048/27/1/015009.
[8] M. Mändl, H. Hoffmann, and P. Kücher, “Diffusion barrier properties of Ti/TiN investigated by transmission electron microscopy,” *J Appl Phys*, vol. 68, no. 5, pp. 2127–2132, Sep. 1990, doi: 10.1063/1.346568.
[9] S. Berg and T. Nyberg, “Fundamental understanding and modeling of reactive sputtering processes,” Apr. 08, 2005, *Elsevier*. doi: 10.1016/j.tsf.2004.10.051.
[10] X. Liu *et al.*, “Superconducting micro-resonator arrays with ideal frequency spacing,” *Appl Phys Lett*, vol. 111, no. 25, Dec. 2017, doi: 10.1063/1.5016190/904922.
[11] D. Lundin and K. Sarakinos, “An introduction to thin film processing using high-power impulse magnetron sputtering,” *J Mater Res*, vol. 27, no. 5, pp. 780–792, 2012, doi: 10.1557/jmr.2012.8.
[12] A. P. Ehiasarian, A. Vetushka, Y. A. Gonzalvo, G. Sfrn, L. Székely, and P. B. Barna, “Influence of high power impulse magnetron sputtering plasma ionization on the microstructure of TiN thin films,” *J Appl Phys*, vol. 109, no. 10, May 2011, doi: 10.1063/1.3579443.
[13] Z.-Y. Yang, Y.-H. Chen, B.-H. Liao, and K.-P. Chen, “Room temperature fabrication of titanium nitride thin films as plasmonic materials by high-power impulse magnetron sputtering,” *Opt Mater Express*, vol. 6, no. 2, p. 540, Feb. 2016, doi: 10.1364/ome.6.000540.
[14] M. C. Burton, A. D. Palczewski, C. E. Reece, and A.-M. Valente-Feliciano, “Progress with Nb Hipims Films on 1.3 GHz Cu Cavities,” in *International Conference on RF Superconductivity*, P. Michel, A. Arnold, and V. R. W. Schaa, Eds., in 19. Dresden, Germany: JACoW Publishing, 2019, pp. 823–827. doi: doi:10.18429/JACoW-SRF2019-THFUB2.
[15] S. Leith *et al.*, “HiPIMS deposition of superconducting Nb thin films onto Cu substrates,” *Vacuum*, vol. 212, p. 112041, Jun. 2023, doi: 10.1016/J.VACUUM.2023.112041.
[16] F. Avino *et al.*, “Improved film density for coatings at grazing angle of incidence in high power impulse magnetron sputtering with positive pulse,” *Thin Solid Films*, vol. 706, p. 138058, Jul. 2020, doi: 10.1016/J.TSF.2020.138058.
[17] A. I. Buzdin, “Proximity effects in superconductor-ferromagnet heterostructures,” *Rev Mod Phys*, vol. 77, no. 3, pp. 935–976, Sep. 2005, doi: 10.1103/RevModPhys.77.935.
[18] A. Anders, “Physics of arcing, and implications to sputter deposition,” *Thin Solid Films*, vol. 502, no. 1–2, pp. 22–28, Apr. 2006, doi: 10.1016/J.TSF.2005.07.228.
[19] D. Carter, H. Walde, and K. Nauman, “Managing arcs in large area sputtering applications,” *Thin Solid Films*, vol. 520, no. 12, pp. 4199–4202, Apr. 2012, doi: 10.1016/J.TSF.2011.04.103.
[20] M. R. Vissers *et al.*, “Characterization and in-situ monitoring of sub-stoichiometric adjustable superconducting critical temperature titanium nitride growth,” *Thin Solid Films*, vol. 548, pp. 485–488, Dec. 2013, doi: 10.1016/j.tsf.2013.07.046.
[21] G. Coiffard *et al.*, “Uniform Non-stoichiometric Titanium Nitride Thin Films for Improved Kinetic Inductance Detector Arrays,” *J Low Temp Phys*, vol. 184, no. 3–4, pp. 654–660, 2016, doi: 10.1007/s10909-016-1489-9.
[22] A. Anders, “Tutorial: Reactive high power impulse magnetron sputtering (R-HiPIMS),” *J Appl Phys*, vol. 121, no. 17, p. 171101, Mar. 2017, doi: 10.1063/1.4978350.
[23] M. R. Vissers *et al.*, “Proximity-coupled Ti/TiN multilayers for use in kinetic inductance detectors,” *Appl Phys Lett*, vol. 102, no. 23, p. 232603, Jun. 2013, doi: 10.1063/1.4804286.
[24] D. Morozov *et al.*, “Design and Characterisation of Titanium Nitride Subarrays of Kinetic Inductance Detectors for Passive Terahertz Imaging,” *J Low Temp Phys*, vol. 193, no. 3, pp. 196–202, 2018, doi: 10.1007/s10909-018-2023-z.